frontiers in Energy Research

ORIGINAL RESEARCH
published: 26 November 2020
doi: 10.3389/fenrg.2020.614621

Mathematical Modeling and Optimization Studies by Artificial Neural Network, Genetic Algorithm and Response Surface Methodology: A Case of Ferric Sulfate–Catalyzed Esterification of Neem (*Azadirachta indica*) Seed Oil

*Kelechi E. Okpalaeke[1], Taiwo H. Ibrahim[2,3], Lekan M. Latinwo[4] and Eriola Betiku[2,4]**

[1]Institute of Ecology and Environmental Studies, Obafemi Awolowo University, Ile-Ife, Nigeria, [2]Biochemical Engineering Laboratory, Department of Chemical Engineering, Obafemi Awolowo University, Ile-Ife, Nigeria, [3]National Biotechnology Development Agency, Abuja, Nigeria, [4]Department of Biological Sciences, Florida Agricultural and Mechanical University, Tallahassee, FL, United States

High free fatty acids (FFA) content in oils poses challenges such as soap formation and difficulty in the separation of by-products in direct transesterification of oil to biodiesel, which is of environmental concern and also increases the cost of production. Thus, in this study, the ferric sulfate-catalyzed esterification of neem seed oil (NSO) with an FFA of 5.84% was investigated to reduce it to the recommended level of ≤1%. The esterification process for the NSO was modeled using response surface methodology (RSM) and artificial neural network (ANN). The effect of the pertinent process input variables *viz.* methanol/NSO molar ratio (10:1–30:1), ferric sulfate dosage (2–6 wt%), and reaction time (30–90 min) and their interactions on the reduction of the FFA of the NSO, were examined using Box Behnken design. The optimal condition for the process for reducing the FFA content of the oil was established using RSM and ANN-genetic algorithm (ANN-GA). The results showed that the models developed described the process accurately with the coefficient of determination (R^2) of 0.9656 and 0.9908 and the mean relative percent deviation (MRPD) of 6.5 and 2.9% for RSM and ANN, respectively. The ANN-GA established the optimum reduction of FFA of 0.58% with methanol/NSO molar ratio of 18.51, ferric sulfate dosage of 6 wt%, and reaction time of 62.8 min as against the corresponding values of 0.62% FFA, 23.5, 5.03, and 75 min established by the RSM. Based on the statistics considered in the study, ANN and GA outperformed RSM in modeling and optimization of the NSO esterification process.

Keywords: plant oil, esterification, neural networks, modeling, optimization, neem oil, response surface methodology, genetic algorithm

OPEN ACCESS

Edited by:
Sachin Kumar,
Sardar Swaran Singh National Institute of Renewable Energy, India

Reviewed by:
Shashi Kant Bhatia,
Konkuk University, South Korea
Eeshan Kalita,
Tezpur University, India

****Correspondence:***
Eriola Betiku
ebetiku@oauife.edu.ng
eriola.betiku@famu.edu

Specialty section:
This article was submitted to Bioenergy and Biofuels, a section of the journal Frontiers in Energy Research

Received: *06 October 2020*
Accepted: *03 November 2020*
Published: *26 November 2020*

Citation:
*Okpalaeke KE, Ibrahim TH, Latinwo LM and Betiku E (2020) Mathematical Modeling and Optimization Studies by Artificial Neural Network, Genetic Algorithm and Response Surface Methodology: A Case of Ferric Sulfate–Catalyzed Esterification of Neem (*Azadirachta indica*) Seed Oil. Front. Energy Res. 8:614621. doi: 10.3389/fenrg.2020.614621*

INTRODUCTION

In the past decade, considerable attention has been focused on renewable and sustainable alternative fuel by various governments and the scientific community because of the finite nature of fossil-based fuels, insecurity of supply, and attendant environmental concerns (Rashid et al., 2011; Merlin et al., 2015). Biodiesel is a potential alternative fuel considered as a credible replacement or supplement to fossil-based fuels in transportation and internal combustion engines (Sani et al., 2013). It is non-toxic, biodegradable, produces less combustion emission, and its usage in internal combustion engines does not require engine modifications (Niu et al., 2018; Ofoefule et al., 2019). Transesterification of triacylglycerides (from plant oils or animal fats or lipids from microalgae) and low molecular weight alcohol (methanol or ethanol) in the presence of a catalyst is the most commonly employed technology for biodiesel production (Gardy et al., 2017; Shan et al., 2018). Traditionally, most biodiesel production processes use refined vegetable oils as feedstock, which are expensive, often push up production cost (Marchetti, 2013; Karmee et al., 2015), and lead to food-energy competition (Betiku and Adepoju, 2013). Since the cost of feedstock accounts for 75–80% of the total operating cost of biodiesel production (Lisboa et al., 2014), lots of research efforts are focusing on the exploration of cheaper, non-edible feedstock alternatives (Rincón et al., 2014).

Previous studies have considered cheap alternatives such as waste cooking oil (Avinash and Murugesan, 2017), sorrel oil (Betiku and Ishola, 2020), rubber seed oil (Oladipo and Betiku, 2020), neem seed oil (NSO) (Merlin et al., 2015; Akhabue et al., 2020), African pear seed oil (Ofoefule et al., 2019), and Jatropha oil (Kamel et al., 2018). A key drawback of this feedstock, however, is their high free fatty acids (FFA) content that has to be reduced to ≤1% via acid-catalyzed esterification process (Gan et al., 2010). High FFA (>1%) favors soap formation (saponification) at the expense of transesterification, thereby leading to low biodiesel yield and difficult product separation (Betiku et al., 2016). Therefore, esterification of several non-edible plant oils with high FFA has been vigorously studied using homogeneous catalysts such as H_2SO_4 (Kamel et al., 2018; Oladipo and Betiku, 2020). Although the reaction with homogeneous catalysts is fast and effective, the catalysts cannot be recycled (that is recovered and reused), which raises both environmental and high cost of biodiesel production concerns. To overcome this challenge, solid heterogeneous catalysts such as ferric sulfate (Gan et al., 2010; Betiku et al., 2017; Ighose et al., 2017; Ishola et al., 2017) and biomass-based materials such as *Hura crepitans* seed pod (Ogbu et al., 2018; Akhabue et al., 2020) have been proposed as possible replacements for homogeneous catalysts since they can be recovered and reused, making them environmentally benign and cost-effective in the production of biodiesel. Past reports have shown that the process input variables *viz.* alcohol/oil molar ratio, catalyst dosage, reaction time, and reaction temperature have significant effects on the reduction of FFA content of the oil through modeling of the esterification process (Betiku et al., 2015; Selvaraj et al., 2019).

Response surface methodology (RSM) is a statistical tool used for experimental design, modeling, and optimization of processes leading to acceptable results from a reduced number of experiments and cost (Betiku et al., 2014). The tool analyzes all possible individual and interactive effects of the independent process factors (numeric or categoric) on the chosen response variable(s) and then develops a regression quadratic model to describe the process. Application of RSM in the design, modeling, and optimization of oil extraction, esterification, and transesterification processes are well documented (Jaliliannosrati et al., 2013; Halder et al., 2015; Ibrahim et al., 2019). Unlike RSM, artificial neural network (ANN) is a collection of biologically inspired (simplified model of human brains) mathematical techniques designed for machine learning, regression, and statistical analysis of often complex data (Shanmuganathan, 2016). It is a reliable alternative to RSM (Betiku et al., 2014) with application in such areas as signal processing, pattern matching, image recognition, language processing, data mining, process modeling, and optimization (Abiodun et al., 2018). This computational tool consists of neuronal structure (neurons as processing elements and synaptic weights attached to the connections between neurons) to which a series of training and recall algorithms are attached. Feedforward and feedback neural network architectures are the more preferred network topology for reasons of processing speed, scalability, fault tolerance, and performance (Mozaffari et al., 2019). Its application to the modeling and optimization of biodiesel production has been investigated (Samuel and Okwu, 2019; Selvaraj et al., 2019).

Neem tree (*Azadirachta indica*) is a tropical evergreen tree that is native to Southeast Asia and is ubiquitous in the northern and western parts of Nigeria. Its seeds contain 25–45% non-edible oil, which has potential as a feedstock for biodiesel production via transesterification (Muthu et al., 2010; Oladipo et al., 2018). However, the presence of FFA >1% means that a pretreatment step via esterification is required (Akhabue et al., 2020). While some studies separately modeled the esterification and transesterification of NSO in a two-step biodiesel production process and then determined the optimum condition for maximum FFA reduction and biodiesel yield using either RSM or ANN for each step (Chhabra et al., 2020), others lumped the two processes together in their modeling and optimization studies (Oladipo et al., 2018) and simply determined the optimum biodiesel yield. There is a dearth of information in the literature on the comparison of modeling and optimization of the esterification process for neem oil with RSM, ANN, and genetic algorithm (GA), which is the aim of this current work.

Hence, this work focused solely on the ferric sulfate-catalyzed esterification of the oil from neem seeds, which had a high FFA as a pretreatment step. Also, the study evaluated the performance of RSM and ANN in the modeling of the esterification process. The effect of the pertinent individual process input variables (alcohol/oil molar ratio, catalyst dosage, and reaction time) and their interactions on the reduction of the FFA of the oil was investigated using a combination of Box Behnken design (BBD) and RSM. The best-operating conditions for the minimization of the percent FFA were established using both RSM and GA.

TABLE 1 | Independent factors and levels investigated.

Factor	Unit	Levels		
		−1	0	+1
Methanol/NSO molar ratio (X_1)	—	10	20	30
Ferric sulfate dosage (X_2)	wt%	2	4	6
Reaction time (X_3)	min	30	60	90

MATERIALS AND METHODS

Materials

The crude NSO used in this study was obtained from the National Research Institute for Chemical Technology in Zaria, Kaduna State, Nigeria. All chemicals and reagents used in this study are all analytical grade *viz*. methanol (99.8%), ethanol (99.7%), diethyl ether (99%), sulfuric acid (98%), ferric sulfate, Wij's solution, potassium hydroxide, and phenolphthalein manufactured by J.T. Baker (Phillipsburg, NJ, United States), BDH Chemicals., Poole England and GFS Chemicals, Inc., Columbus, OH, United States).

Methods

Neem Seed Oil Quality Characterization

The physicochemical and fuel properties of the NSO were determined using the AOAC protocols (AOAC, 1990). The acid value and %FFA were calculated for the crude and esterified NSO using **Eqs. 1**, **2**, respectively in which V represents the volume of potassium hydroxide used during titration, and N is the normality of the same.

$$\text{Acid Value}\left(\text{mg}\frac{\text{KOH}}{\text{g oil}}\right) = \frac{V^{*}\,N^{*}\,56.1}{\text{Weight of oil sample}} \quad (1)$$

$$\%\ \text{FFA} = \text{Acid value}/1.99 \quad (2)$$

Description of the Esterification Process

Based on the experimental design, specific volume of the NSO was measured into a 500-ml three-necked glass flask which served as the reactor and was heated to a temperature of 100°C on a magnetic stirrer with a hot plate. Methanol was then added to the oil in the reactor and was allowed to mix for 5 min after ferric sulfate was added to the mixture. The temperature of the reaction was maintained at 65°C. At the end of the reaction, the product was transferred into a separating funnel, which was allowed to stand for 2 h. The surplus methanol left in the esterified NSO was removed via heating (Ishola et al., 2017).

Experimental Design, Model Development, and Optimization by Response Surface Methodology

In this study, the effects of process variables *viz*. methanol/NSO molar ratio, ferric sulfate dosage, and reaction time on the %FFA as the response variable, and mutual interactions, were examined by a three-level-three-factor BBD. **Table 1** shows coded independent factors with their levels, which were used to produce 17 experimental conditions randomly executed in the laboratory. A second-order polynomial equation (**Eq. 3**) was regressed to develop the model for predicting the response variable (%FFA).

$$Y = \propto_o + \propto_1 X_1 + \propto_2 X_2 + \propto_3 X_3 + \propto_{12} X_1 X_2 + \propto_{13} X_1 X_3 + \propto_{23} X_2 X_3 + \propto_{11} X_1^2 + \propto_{22} X_2^2 + \propto_{33} X_3^2 \quad (3)$$

where, Y represents the predicted response (%FFA); α_o is the intercept term; α_1, α_2, α_3 are the linear coefficients; α_{12}, α_{13}, α_{23} are the interaction coefficients; α_{11}, α_{22}, α_{33} are the quadratic coefficients; and X_1, X_2, X_3 are the coded independent variables.

Equation 3 was subjected to multiple regressions to fit the coefficients to experimental data, the performance of the model was evaluated using the analysis of variance (ANOVA) and the test of significance. For the optimization, the desirability function approach was applied to solving the regressed quadratic equation to establish the optimum conditions to achieve the lowest %FFA. These conditions were then mimicked in the model validation experiments conducted in triplicates and the results were averaged and then compared with model-predicted %FFA as a way of assessing the predictive accuracy of the model. All procedures from experimental design, model development, and process optimization were carried out with the aid of the Statistica 10 software package (StatSoft, Inc., Tulsa, OK, United States).

Artificial Neural Network Model Development and Optimization

The modeling of the esterification process for the NSO by ANN was conducted using a feedforward, multilayer architecture, and a back-propagation, learning algorithm that was based on the Levenberg-Marquardt method. While Levenberg-Marquardt was used for data fitting and the number of hidden neurons was determined via iteration by testing several neural networks until the mean square error (MSE) value of the output was minimized, the neurons in the hidden layer are set up to sum up the weighted inputs and its associated bias. The hyperbolic tangent sigmoid (*tansig*) and pure linear (*purelin*) activation transfer function was respectively implemented for the hidden and output layers. Also, 70% of the experimental data was used for network training and 15% each for validation and testing to appraise the ability of the model to predict hidden data not used for training as well as its generalization capability (Ishola et al.,

TABLE 2 | Network configurations/features for the developed model.

Property	Value/Comment
Algorithm	Levenberg-Marquardt back-propagation
Minimised error function	MSE
Learning	Supervised
Input layer	No transfer function is used
Hidden layer	Hyperbolic tangent sigmoid (tansig)
Output layer	Purelin transfer function
Number of training iterations	69
Number of best iterations	51
Number of input neurons	3
Number of hidden neurons	10
Number of output neurons	1

TABLE 3 | Features of the ANN-GA network configuration.

Property	ANN-GA
Population	10–15
Generation	15–55
Selection	Uniform
Mutation rate	0.1
Cross over rate	0–1
Cross over function	Constraint dependent

2019; Betiku and Ishola, 2020). Furthermore, optimization of the process variables was carried out by coupling the ANN model with the GA. Details of the network configurations for the modeling and ANN-GA optimization are respectively shown in **Tables 2**, **3**.

Sensitivity Analysis of Process Input Variables

For the RSM investigation, **Eq. 4** was used to determine the influence of each input variable on the model based on the sum of squares (Ishola et al., 2019; Betiku and Ishola, 2020). While for ANN, the contribution level of each input variable was determined by Garson (1991) method as described by **Eq. 5**.

$$\text{Contribution of input variable } (\%) = \frac{\text{Sum of squares of variable}}{\text{Sum of squares for all variables}} \quad (4)$$

$$S_j = \sum_{m=1}^{m=n_h}\left(\left(\frac{\left|w_{jm}^{ih}\right|}{\sum_{k=1}^{n_i}\left|w_{km}^{ih}\right|}\right)\times\left|w_{mn}^{ho}\right|\right)\Bigg/\sum_{k=1}^{k=n_i}\left[\sum_{m=1}^{m=n_h}\left(\left(\frac{\left|w_{km}^{ih}\right|}{\sum_{k=1}^{n_i}\left|w_{km}^{ih}\right|}\right)\times\left|w_{mn}^{ho}\right|\right)\right] \quad (5)$$

where, S_j is the significance of the jth input variable on the output response. n_h and n_i are the number of hidden and input neurons, respectively. w represents the weight, while i, h, and o are the layers representing input, hidden, and output, respectively. k, m, and n represent input, hidden and output neurons, respectively.

Performance Assessment of Models

The two models obtained by RSM and ANN were subjected to statistical analysis to determine their effectiveness (**Table 4**). Statistics such as the correlation coefficient (R), coefficient of determination (R^2), Adjusted R^2, MSE, root MSE (RMSE), mean average error, standard error of prediction, mean relative percent deviation (MRPD). The details of the equations for determining the parameters have been described in our previous works (Betiku et al., 2016; Ishola et al., 2019).

RESULTS AND DISCUSSION

Physicochemical Properties of Neem Seed Oil

The properties of the NSO used in this work are presented in **Table 4**. At room temperature, the NSO was a dark brownish colored liquid with a density of 947.9 kg/m^3. The acid value (11.67 mg KOH/g oil) and FFA (5.94%) of the NSO differ from those reported in the literature (Akhabue et al., 2020; Chhabra et al., 2020). These may be due partly to the source of the seeds or the hydrolysis of the triglycerides. But the values are generally too high for one-step transesterification (Chhabra et al., 2020). These should be reduced to <2.0 mg KOH/g oil or ≤1% FFA to avoid soap formation and also ease the glycerine separation during biodiesel production (Betiku et al., 2014). The saponification value of 186.53 mg KOH/g oil is high, indicating the tendency of NSO to form soap. The kinematic viscosity of 21.38 mm^2/s suggests that the NSO is highly viscous and may tend to flow slowly due to this resistance to flow. The iodine value of 73.21 g I_2/100 g points to a high level of unsaturation of fatty acids in the NSO. The acid value of 11.67 mg KOH/g oil of the NSO indicates that the oil requires s lots of alkali for its neutralization. The peroxide value of 1.53 meq/g oil suggests that the oil is not prone to rancidity, which means it has a long shelf life (Jisieike and Betiku, 2020). A value of 59.09 for cetane number indicates the aptness of NSO as a potential feedstock with good fuel quality.

The fatty acids present in the NSO as previously reported in our past work are palmitic (18.1%), stearic (18.1%), oleic (44.5%), linoleic (18.3%), linolenic (0.2%) and arachidic (0.8%) (Betiku et al., 2014). The functional groups present in the NSO were identified using Fourier transform infrared technique. The spectrum obtained with the identified functional groups is shown in **Figure 1**. The presence of –C=O (ester) overtone is identified by the weak band located at 3,443 cm^{-1} (Guillén and Cabo, 1998). The strong bands at 2,926 and 2,854 cm^{-1} represent the asymmetric and symmetric stretching vibrations of –C–H in CH_2 group, respectively (Okeleye and Betiku, 2019). The typical –C=O stretching vibration of the carbonyl group present in triglycerides, is illustrated by the strong band located at 1,745 cm^{-1} (Guillén and Cabo, 1998; Coates, 2000; Okeleye and Betiku, 2019). The bands located at 1,465, 1,379, 1,240, 1,165, and 1,030 cm^{-1} in the fingerprint region of triglycerides indicate the presence of –C–H (CH_2) bending (scissoring), –C–H

TABLE 4 | Physical and chemical properties of crude NSO.

Properties	Unit	Methods	Values
Physical state at room temperature	—	Visual	Liquid/dark brown
Moisture content	%	(AOAC, 1990)	1.6129 ± 0.00
pH	—	(AOAC, 1990)	6.84 ± 0.01
Kinematic viscosity at 40°C	mm^2/s	(AOAC, 1990)	21.38 ± 0.02
Density at room temperature	(kg/m^3)	(AOAC, 1990)	947.90 ± 0.45
Refractive index	—	(AOAC, 1990)	1.48 ± 0.00
Saponification value	mg KOH/g oil	(AOAC, 1990)	186.53 ± 1.40
Iodine value	g I_2/100 g	(AOAC, 1990)	73.21 ± 0.39
Acid value	Mg KOH/ g oil	(AOAC, 1990)	11.67 ± 0.09
FFA	%	(AOAC, 1990)	5.84 ± 0.05
Peroxide value	meq/g oil	(AOAC, 1990)	1.53 ± 0.25
Calorific value	(MJ/kg)	(Demirbaş, 1998)	40.68 ± 0.05
Cetane number	—	(Krisnangkura, 1986)	59.08 ± 0.08

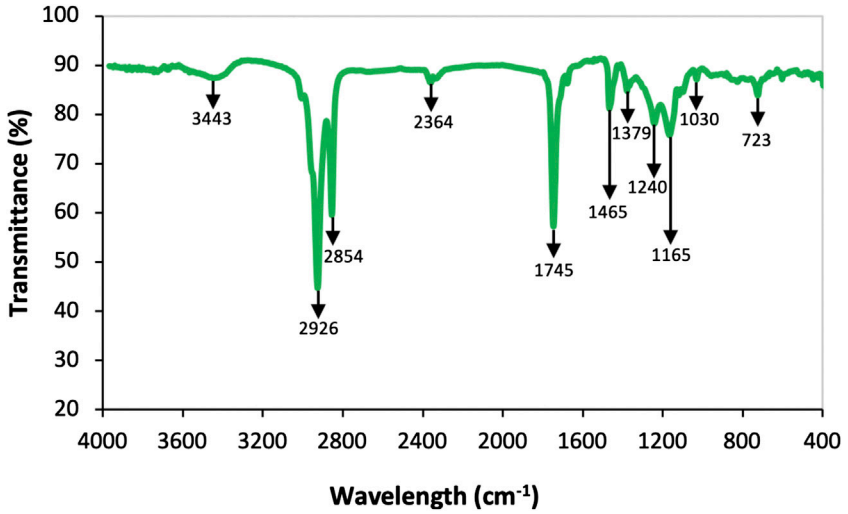

FIGURE 1 | FTIR spectrum for the NSO.

TABLE 5 | Design matrix, experimental and predicted values of %FFA.

Run no	Methanol/NSO molar ratio	Ferric sulfate dosage (wt%)	Reaction time (min)	Experimental FFA (%)	RSM predicted FFA (%)	ANN predicted FFA (%)
1	20	4	60	0.8265	0.838	0.827
2	20	6	30	0.858	1.007	0.823
3	10	2	60	1.994	2.047	1.870
4	10	4	30	2.031	1.968	2.030
5	20	6	90	0.7825	0.773	0.783
6	30	4	30	1.027	0.931	0.990
7	20	4	60	0.894	0.838	0.827
8	30	6	60	0.7895	0.736	0.790
9	20	4	60	0.893	0.838	0.827
10	30	2	60	1.049	1.135	1.050
11	20	4	60	0.7635	0.838	0.827
12	20	2	90	1.232	1.083	1.200
13	20	4	60	0.8111	0.838	0.827
14	10	4	90	1.248	1.344	1.260
15	10	6	60	1.5585	1.472	1.580
16	20	2	30	1.662	1.671	1.610
17	30	4	90	0.6705	0.733	0.660

(CH_3) bending (symmetric), –C–O, –CH_2 (stretching, bending), strong –C–O, –CH_2 – (stretching, bending) and –C–O (stretching), respectively (Guillén and Cabo, 1998; Coates, 2000; Okeleye and Betiku, 2019). The band located at 723 cm^{-1} indicated the presence of bending out of – HC = CH – (cis) and rocking vibration of $(CH_2)_n$ (Guillén and Cabo, 1998; Coates, 2000).

Process Modeling of Neem Seed Oil Esterification Results

Response Surface Methodology Model Description

Results from the ferric sulfate-catalyzed esterification of NSO as a pretreatment step in biodiesel production with the experimental conditions generated from the BBD are shown in **Table 5**. The NSO used and the esterified NSO together with the byproducts, that is, glycerol, excess methanol, and the catalyst, are displayed in **Figure 2**. **Eq. 6** is the quadratic model equation developed via RSM to correlate the response variable (%FFA) to the independent variables in terms of the coded values. From **Table 5**, it can be seen that all the experimental conditions generated by the BBD and subsequently used to conduct experiments in the laboratory all led to significant reductions in the %FFA of the NSO.

$$Y = 5.942 - 0.195X_1 - 0.654X_2 - 0.033X_3 + 0.002X_1X_2 + 0.0004X_1X_3 + 0.0012X_2X_3 + 0.003X_1^2 + 0.05X_2^2 + 0.0001X_3^2 \quad (6)$$

FIGURE 2 | NSO and separation of esterified NSO from byproducts.

TABLE 6 | Univariate test of significance for regression coefficients and ANOVA.

Source	SS	df	MS	F-value	*p*-value
Significance test					
X_1 (Methanol/NSO molar ratio)	1.3575	1	1.3575	91.3767	0.00003
X_2 (Ferric sulfate dosage)	0.4746	1	0.4746	31.9443	0.00077
X_3 (Reaction time)	0.3382	1	0.3382	22.7680	0.00203
X_1X_2	0.0077	1	0.0077	0.5212	0.49371
X_1X_3	0.0455	1	0.0455	3.0610	0.12367
X_2X_3	0.0314	1	0.0314	2.1147	0.18921
X_1^2	0.4054	1	0.4054	27.2913	0.00122
X_2^2	0.1681	1	0.1681	11.3155	0.01202
X_3^2	0.0389	1	0.0389	2.6223	0.14937
Error	0.103996	7	0.1014857	—	—
Total SS	3.027403	16	—	—	—
ANOVA					
Model	2.9234	9	0.32482	21.86399	0.000255
R^2	0.9656	—	—	—	—
Adjusted R^2	0.9215	—	—	—	—

SS, sum of squares; df, degree of freedom; MS, mean square.

Fit Statistics for the Response Surface Methodology Model

The ANOVA results indicated that the quadratic mathematical model obtained in this work is significant at p-value < 0.05 (**Table 6**). The goodness of fit of the regression model was assessed by calculating the R and R^2. The value of R (0.9826) of the model shows good agreement between the predicted and experimental values, which was also confirmed by the parity plot in **Figure 3**. The R^2 of 0.9656 suggests that only 3.44% of the total variation in the response is not described by the model (Betiku and Ajala, 2014). The adjusted R^2 (0.9215) and the predicted R^2 (0.9656) obtained showed that the values are in reasonable agreement with each other with an acceptable difference of 0.0441 (the maximum allowable difference is 0.2), which also shows the capability of the model to predict the response adequately. The model F-value of 21.86 and the p-value of ˂0.0003 imply that the model was statistically significant at a 95% confidence level (p < 0.05).

The F-value of 9.70 and the p-value of ˂0.0262 imply the lack of fit is not significant relative to the pure error, which is desirable (**Table 6**). Also, the individual model terms were also tested using ANOVA at a 95% confidence level (p < 0.05), based on both the p-value and F-value, all the terms were significant except X_1X_2 (interaction between methanol/NSO molar ratio and ferric sulfate dosage), X_1X_3 (interaction between methanol/NSO molar ratio and reaction time), X_2X_3 (interaction between ferric sulfate dosage and reaction time), $X_2{}^2$ (quadratic of ferric sulfate dosage) and X_3^2 (quadratic of reaction time). Adequate precision is generally used to measure the signal to noise ratio and a ratio greater than 4 is desirable. The ratio of 14.057 indicates an adequate signal, which shows that the model can be used to navigate the design space. **Figure 4** displays the Pareto chart with the level of significance of all the model terms on the % FFA reduction. The length of each bar indicates the significance level of the variable it represents, any bar behind the reference line (p = 0.05) denotes insignificance (Ishola et al., 2017). The chart shows that five out the total of nine model terms were significant at p < 0.05.

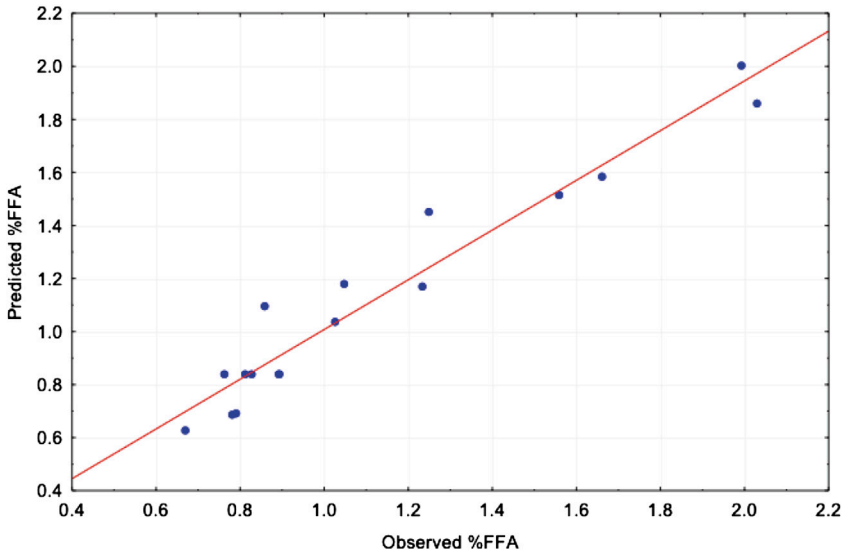

FIGURE 3 | Parity plot for the actual and predicted values of % FFA for RSM model.

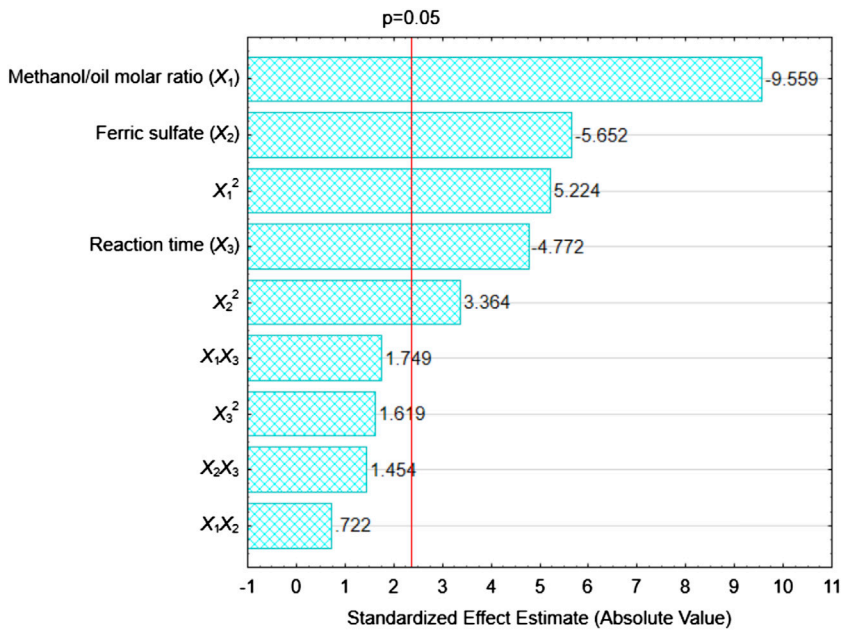

FIGURE 4 | Pareto chart indicating significant level for all model terms.

The chart shows that the linear term of methanol/NSO molar ratio was the most significant model term followed by the linear term of ferric sulfate dosage, the quadratic of methanol/NSO molar ratio, reaction time, and the quadratic of ferric sulfate dosage. Conversely, all the interaction terms and the quadratic of the reaction time are all insignificant. This observation is supported by the test of significance presented in **Table 6**.

The interactions among the process variables were investigated by the contour (2-D) and response surface (3-D) plots using the Statistica 10 software package (**Figure 5**). The effect of methanol/NSO molar ratio and ferric sulfate dosage on the FFA of the NSO is displayed in **Figure 5A**. As the methanol/NSO molar ratio increases with increasing ferric sulfate dosage, the %FFA decreases significantly. The lowest %FFA was observed at ferric sulfate dosage of 5.5 wt% and methanol/NSO molar ratio of 28:1. Beyond this point, %FFA was observed to increase. While **Figure 5B** shows the interactive effect of ferric sulfate dosage and reaction time, the effect of reaction time and methanol/NSO

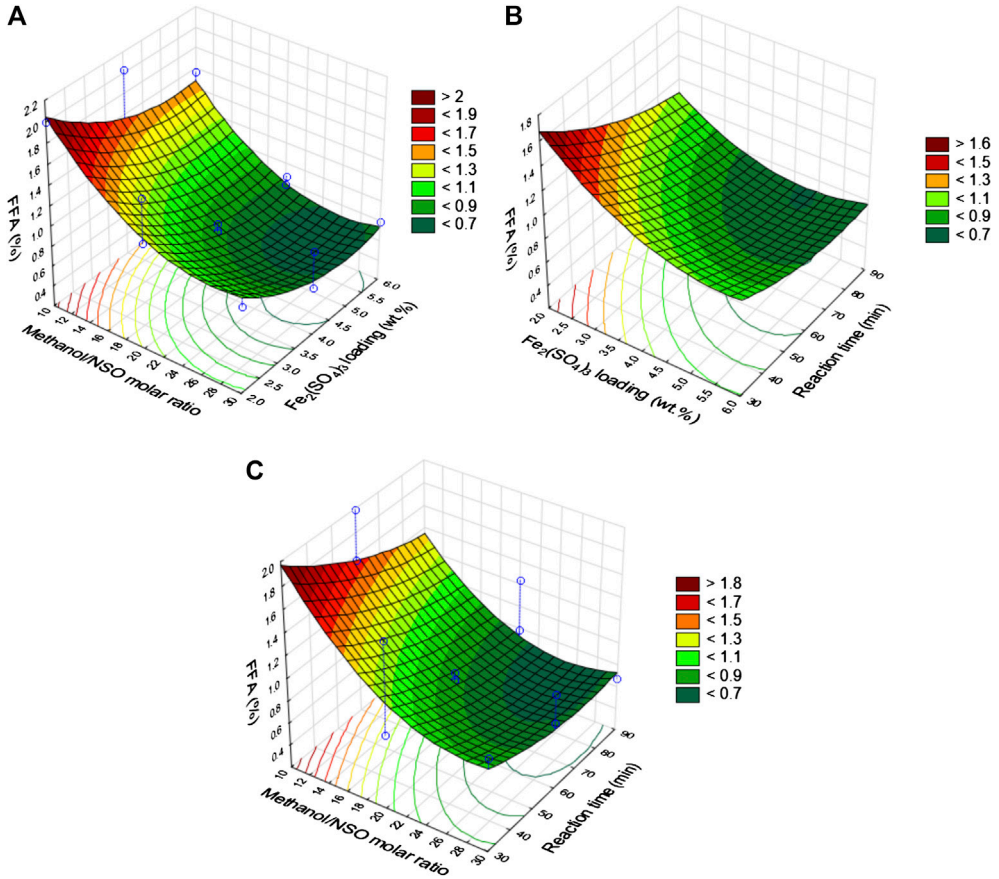

FIGURE 5 | Response surface plots for NSO esterification process. **(A)** methanol NSO molar ratio vs. catalyst loading; **(B)** catalyst loading vs. reaction time and **(C)** methanol NSO molar ratio vs. reaction time.

molar ratio on %FFA is displayed in **Figure 5C**. **Figure 5C** shows that the interaction of the variables has a significant effect on the %FFA.

%FFA was observed to be <0.7 at methanol/NSO molar ratio of 28:1 and reaction time of 90 min. Further increase in methanol/NSO molar ratio beyond 28:1 was observed to cause an increase in the %FFA. The nature of the curvature of the three plots demonstrates that the three process input variables have a significant influence on the FFA reduction. Esterification of oil with alcohol is a reversible reaction controlled by the equilibrium of the reaction (Pasias et al., 2006); thus, the alcohol/oil molar ratio should be greater than the stoichiometric requirement to have a high reduction of the FFA of the oil (Marchetti and Errazu, 2008). This is evident in **Figures 5A,B** since the %FFA decreases as the methanol/NSO molar ratio increases. This observation is corroborated by the reports on esterification of castor oil (Karmakar et al., 2018) and NSO (Betiku et al., 2017). The influence of the ferric sulfate dosage on the reduction of % FFA followed a similar trend with the methanol/NSO molar ratio, but the reaction time had less effect (**Figure 5**).

Artificial Neural Network Model Description

After several trials, the best network structure chosen for the ANN modeling of the NSO esterification process consisted of an input layer of three neurons (methanol/NSO molar ratio, ferric sulfate dosage, and reaction time), an output layer of one neuron (%FFA) and a hidden layer of 10 neurons (**Figure 6**). The responses predicted from the ANN model are as presented in **Table 5**. The R values of 0.9996, 0.9978, 0.9921, and 0.9954, respectively obtained from the plots of predicted versus experimental values for the training, testing, validation, and whole data sets indicated that there is a good correlation between the experimental and predicted values (**Figure 7**).

Also, the high values confirmed good generalization and predictive capability of the ANN model since it was able to predict the outputs of validation and testing data that were not part of the training set used to develop the model (Sarve et al., 2015; Ishola et al., 2019). The developed ANN model was further evaluated using R^2. The value of 0.9958 suggests that 99.58% of the variations in both the experimental and predicted values can be explained, indicating a good fit of the model (Okeleye and Betiku, 2019). The maximum values of R and R^2 possible are 1.0 and the higher the value the better. A model is deemed acceptable if $R^2 \geq 0.8$ (Myers et al., 2016). The observation made in this work is supported by the ANN modeling of esterification of palm kernel oil using H_2SO_4 as a catalyst, where high values of R and R^2 were also reported (Betiku et al., 2016).

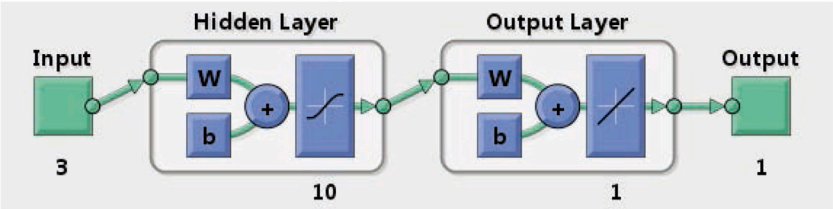

FIGURE 6 | Feedback architecture for the ANN model.

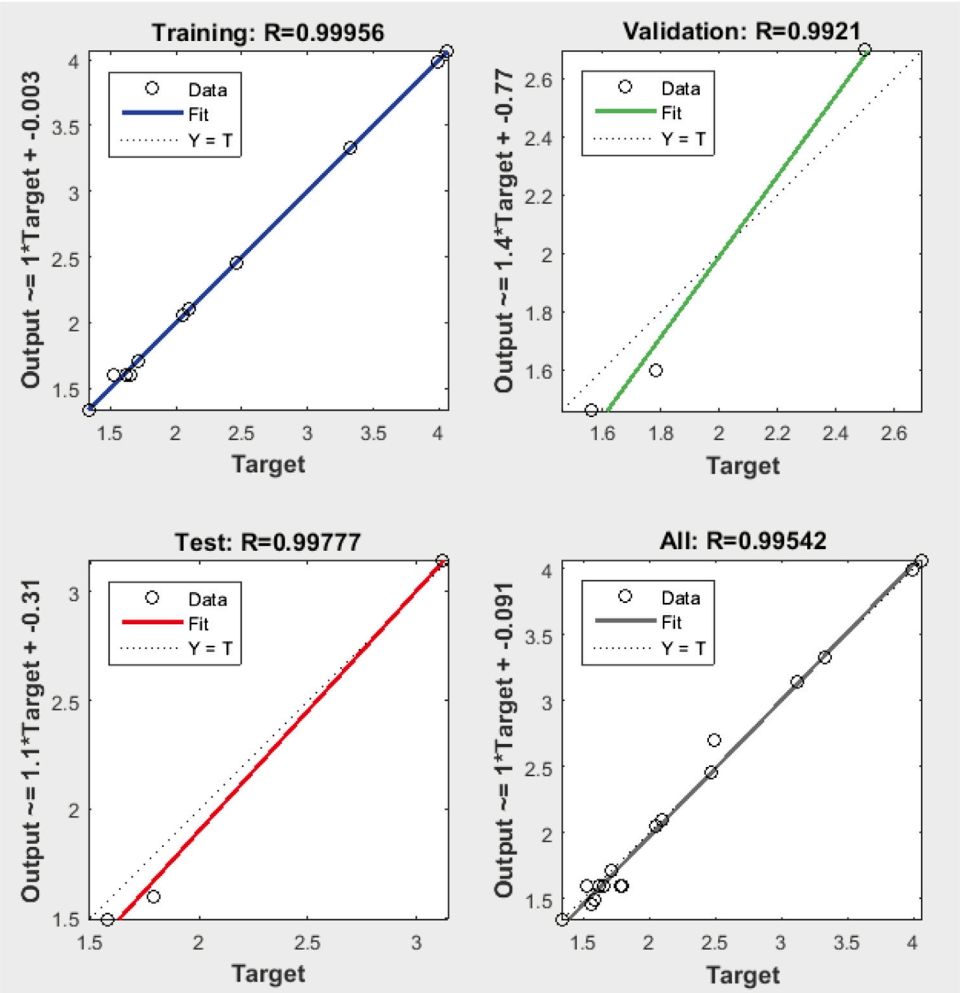

FIGURE 7 | Correlation plots of predicted versus experimental values for the ANN model.

Comparison of Performance of the Developed Models

The comparative performance of the models in terms of predictive accuracy for the esterification of NSO was evaluated using various fit statistics and the results obtained are presented in **Table 7**. The values of R, R^2, and adjusted R^2 observed are very high for models obtained with RSM and ANN, indicating a good fit of the experimental data, though the ANN model had higher values than the RSM model. Also, MSE, root MSE, standard error of prediction, mean average error, and MRPD measure the error in the prediction of a model in comparison to the experimental data data (Okeleye and Betiku, 2019; Selvaraj et al., 2019). The ANN model had much lower error values compared to the RSM model. This observation is corroborated by the plots of the experimental against predicted values based on the R^2 of the models (**Figure 8**). The values predicted by the

TABLE 7 | Comparative performance evaluation of RSM and ANN models.

S/N	Parameter	RSM	ANN
1	R	0.982674	0.995418
2	R^2	0.965649	0.990858
3	Adjusted R^2	0.921482	0.988748
4	MSE	0.006117	0.002091
5	RMSE	0.078214	0.045728
6	MAE	0.066869	0.031759
7	SEP	6.965045	4.072111
8	MRPD	6.51244	2.884038

ANN model aligned closer to the reference line than the values predicted by the RSM model.

To further visualize the performance of the developed models, the observed and predicted values were plotted against the experimental run numbers (**Figure 9**). The predicted values from the ANN model are very close to the experimental data better than the values predicted by the RSM model. Predictions by ANN models were superior to that of RSM models in the esterification of palm kernel oil (Betiku et al., 2016), transesterification of sorrel oil (Ishola et al., 2019), and transesterification of sesame oil (Sarve et al., 2015).

Figure 10 shows the results of the sensitivity analysis for the models. The plot demonstrates the level of influence of each of the independent variables in the model. The results for both RSM and ANN followed the same trend. In both cases, the methanol/NSO molar ratio had the most influence on the %FFA, followed by ferric sulfate dosage and then the reaction time. The influence pattern in the ANN model is similar among the input variables compared to the RSM model. The order of influence exhibited in **Figure 9** is supported by the F-values obtained for the variables. The F-values are 91.3767, 31.9443, and 22.7680 for methanol/NSO molar ratio, ferric sulfate dosage, and reaction time, respectively (**Table 6**).

Establishment of Optimum Conditions and Model Validation

By solving the quadratic model equation (**Eq. 6**), the optimum values for the process input variables for the NSO esterification were determined by the RSM as methanol/NSO molar ratio of 23.5, reaction time of 75 min, and ferric sulfate dosage of 5.03 wt% with predicted %FFA of 0.63. The ANN-GA gave the condition as methanol/NSO molar ratio of 18.51, reaction time of 62.8 min, and ferric sulfate dosage of 6.0 wt.% with predicted %FFA of 0.53. To validate the developed models, the predicted values were used to carry out three independent experiments in the laboratory in each case, and the %FFA obtained were averaged, and the values obtained were reported (**Table 8**). The reaction temperature was kept at 65°C in both cases for the laboratory experiments. The experimental %FFA obtained were 0.62 and 0.58 for RSM and ANN, respectively. The condition predicted by ANN-GA was better than the RSM predicted condition.

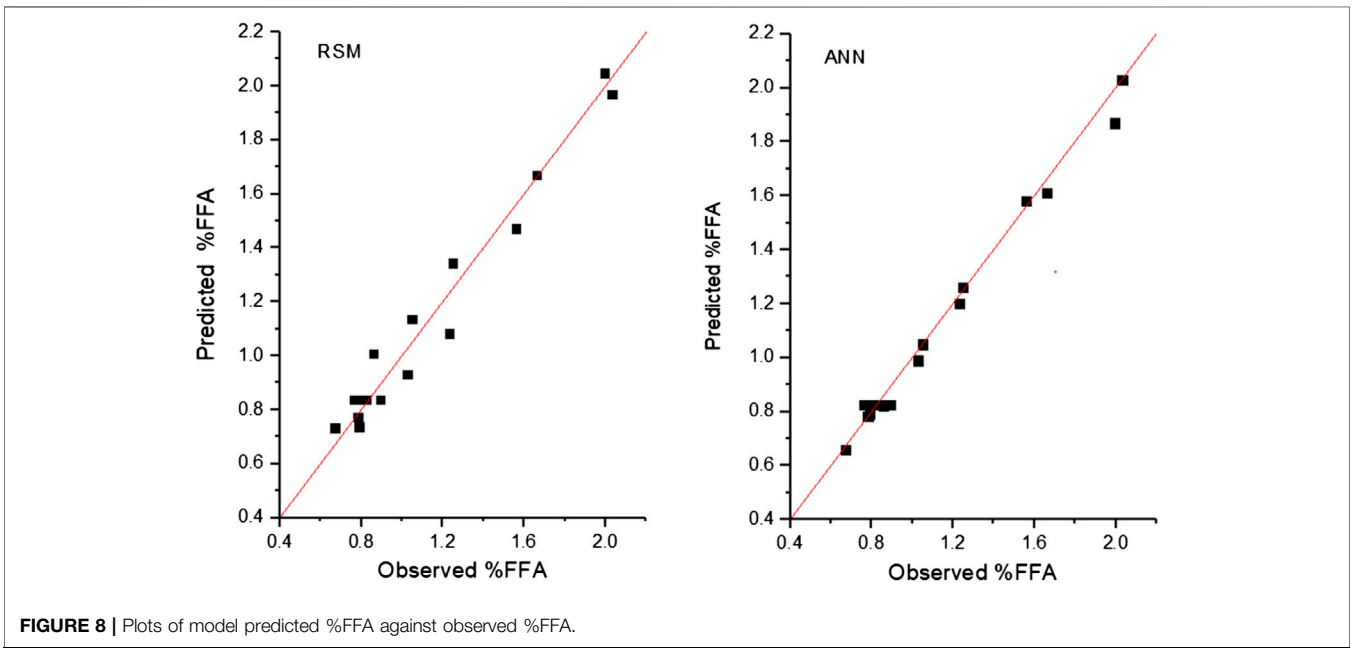

FIGURE 8 | Plots of model predicted %FFA against observed %FFA.

TABLE 8 | Predicted optimization conditions and experimental model validation.

Tool	Methanol/NSO molar ratio	ferric sulfate dosage (wt%)	Reaction time (min)	Predicted FFA (wt%)	Actual FFA (wt%)
RSM	23.50	5.03	75.0	0.63	0.6234 ± 0.02
ANN-GA	18.51	6.00	62.8	0.53	0.5842 ± 0.03

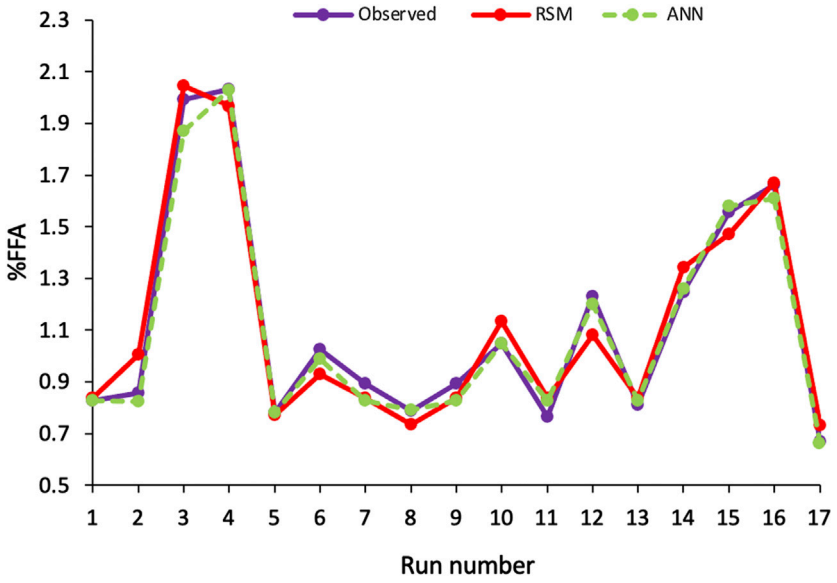

FIGURE 9 | Plots of observed and model predicted %FFA versus experimental run number.

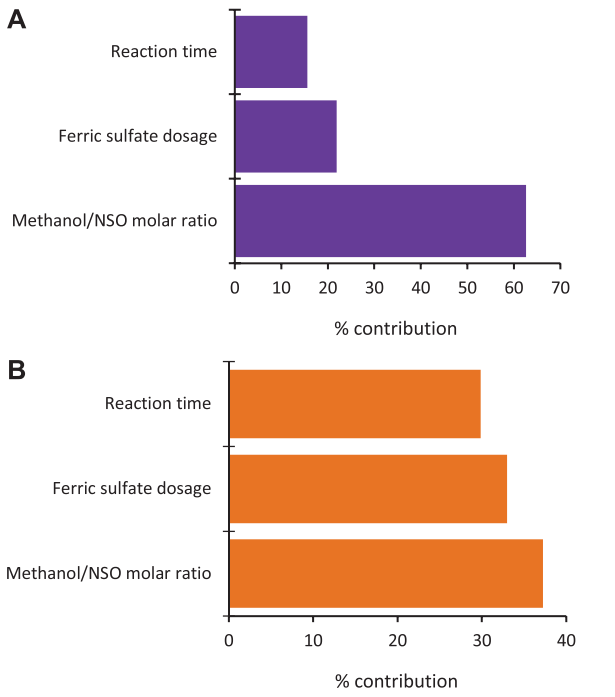

FIGURE 10 | Sensitivity level of input variables, **(A)** RSM and **(B)** ANN.

The superiority of ANN-GA over RSM has been demonstrated in the optimization of process input variables for palm kernel oil esterification (Betiku et al., 2016) and transesterification of sorrel oil (Ishola et al., 2019). Thus, these previous studies support the observation made in this present work. The optimal condition previously established for the esterification of NSO (with an initial acid value of 11.67 mg KOH/g oil) using RSM was the methanol/NSO molar ratio of 2.19 (v/v), reaction time of 15 min, ferric sulfate dosage of 6 wt%, and temperature of 65°C with an acid value of 1.8 mg KOH/g oil which corresponds to %FFA of 0.90 (Betiku et al., 2017). In another study with RSM, the optimum values established for the esterification of NSO (with an initial acid value of 10.18 mg KOH/g oil) was methanol/NSO molar ratio of 0.55 (v/v), reaction time of 36 min, H_2SO_4 dosage of 0.45%, and temperature of 60°C with an acid value of 1.22 mg KOH/g oil which corresponds to %FFA of 0.61 (Betiku et al., 2017).

CONCLUSION

The comparative performance of RSM and ANN to predict the extent of FFA reduction during esterification of NSO, with methanol and ferric sulfate as a solid acid heterogeneous catalyst, was evaluated in this work. Based on the statistics considered, the ANN model with a higher R^2 (0.9909) and a significantly lower MRPD (2.9%) outperformed the RSM model with a lower R^2 (0.9657) and a higher MRPD (6.5%). For the optimization of the process input variables, the minimum FFA (0.53%) was predicted by ANN coupled with GA at a more desired optimal condition of methanol/NSO molar ratio of 18.51, ferric sulfate dosage of 6 wt.%, and reaction time of 62.8 min. The prediction by ANN-GA was better by a margin of 1% FFA of the esterified NSO, which suggests that it can be converted to biodiesel via transesterification without soap formation. Apart from validating the use of the ferric sulfate-catalyzed esterification of NSO as a viable pretreatment step, this work also demonstrated the higher predictive accuracy of the ANN model than the RSM model. Also, GA was shown to be better than RSM as an optimization tool.

DATA AVAILABILITY STATEMENT

The original contributions presented in the study are included in the article/supplementary material, further inquiries can be directed to the corresponding author/s.

AUTHOR CONTRIBUTIONS

Conceptualization, EB; methodology, KEO; software, EB and KEO; validation, KEO; formal analysis, KEO and EB; investigation, KEO; resources, EB and LML; data curation, KEO and EB; writing—original draft preparation, THI; writing—review and editing, KEO, EB, and LML; visualization, KEO and EB; supervision, EB; project administration, EB. All authors contributed and agreed to the published version of the manuscript.

ACKNOWLEDGMENTS

KO acknowledged the technical assistance offered by Mr. Niyi Ishola in this work. EB is thankful to FAMU for creating an enabling environment for the write up of this work.

REFERENCES

Abiodun, E. O., Jantan, A., Dada, K. V., Mohamed, N. A., and Arshad, H. (2018). State-of-theart in artificial neural network applications: a survey. *Heliyon* 4, e00938. doi:10.1016/j.heliyon.2018.e00938

Akhabue, C. E., Osa-Benedict, E. O., Oyedoh, E. A., and Otoikhian, S. K. (2020). Development of a bio-based bifunctional catalyst for simultaneous esterification and transesterification of neem seed oil: modeling and optimization studies. *Renew. Energy* 152, 724–735. doi:10.1016/j.renene.2020.01.103

AOAC (1990). *Official methods of analysis of the association of official analytical chemists*. Washington, VA: AOAC.

Avinash, A., and Murugesan, A. (2017). Economic analysis of biodiesel production from waste cooking oil. *Energy Sources B Energy Econ. Plann.* 12, 890–894. doi:10.1080/15567249.2017.1319438

Betiku, E., and Adepoju, T. F. (2013). Methanolysis optimization of sesame (*Sesamum indicum*) oil to biodiesel and fuel quality characterization. *Int. J. Energy Environ. Eng.* 4, 9. doi:10.1186/2251-6832-4-9

Betiku, E., and Ajala, S. O. (2014). Modeling and optimization of Thevetia peruviana (yellow oleander) oil biodiesel synthesis via Musa paradisiacal (plantain) peels as heterogeneous base catalyst: a case of artificial neural network vs. response surface methodology. *Ind. Crop. Prod.* 53, 314–322. doi:10.1016/j.indcrop.2013.12.046

Betiku, E., Etim, A. O., Pereao, O., and Ojumu, T. V. (2017). Two-step conversion of neem (*Azadirachta indica*) seed oil into fatty methyl esters using a heterogeneous biomass-based catalyst: an example of cocoa pod husk. *Energy Fuels* 31, 6182–6193. doi:10.1021/acs.energyfuels.7b00604

Betiku, E., and Ishola, N. B. (2020). Optimization of sorrel oil biodiesel production by base heterogeneous catalyst from kola nut pod husk: neural intelligence-genetic algorithm versus neuro-fuzzy-genetic algorithm. *Environ. Prog. Sustain. Energy* 39, e13393. doi:10.1002/ep.13393

Betiku, E., Odude, V. O., Ishola, N. B., Bamimore, A., Osunleke, A. S., and Okeleye, A. A. (2016). Predictive capability evaluation of RSM, ANFIS and ANN: a case of reduction of high free fatty acid of palm kernel oil via esterification process. *Energy Convers. Manag.* 124, 219–230. doi:10.1016/j.enconman.2016.07.030

Betiku, E., Okunsolawo, S. S., Ajala, S. O., and Odedele, O. S. (2015). Performance evaluation of artificial neural network coupled with generic algorithm and response surface methodology in modeling and optimization of biodiesel production process parameters from shea tree (*Vitellaria paradoxa*) nut butter. *Renew. Energy* 76, 408–417. doi:10.1016/j.renene.2014.11.049

Betiku, E., Omilakin, O. R., Ajala, S. O., Okeleye, A. A., Taiwo, A. E., and Solomon, B. O. (2014). Mathematical modeling and process parameters optimization studies by artificial neural network and response surface methodology: a case of non-edible neem (*Azadirachta indica*) seed oil biodiesel synthesis. *Energy* 72, 266–273. doi:10.1016/j.energy.2014.05.033

Chhabra, M., Saini, B. S., and Dwivedi, G. (2020). Optimization of the dual stage procedure of biodiesel synthesis from Neem oil using RSM based Box Behnken design. *Energy Sources, Part A Recovery, Util. Environ. Eff.* 1–24. doi:10.1080/15567036.2020.1771480

Coates, J. (2000). "Interpretation of infrared spectra, a practical approach," in *Encyclopedia of analytical chemistry*. Editor R. A. Meyers (Chichester, UK: John Wiley & Sons, Ltd.).

Demirbaş, A. (1998). Fuel properties and calculation of higher heating values of vegetable oils. *Fuel* 77, 1117–1120. doi:10.1016/S0016-2361(97)00289-5

Gan, S., Ng, H. K., Ooi, C. W., Motala, N. O., and Ismail, M. A. F. (2010). Ferric sulphate catalysed esterification of free fatty acids in waste cooking oil. *Bioresour. Technol.* 101, 7338–7343. doi:10.1016/j.biortech.2010.04.028

Gardy, J., Hassanpour, A., Lai, X., Ahmed, M. H., and Rehan, M. (2017). Biodiesel production from used cooking oil using a novel surface functionalised TiO2 nano-catalyst. *Appl. Catal. B Environ.* 207, 297–310. doi:10.1016/j.apcatb.2017.01.080

Garson, G. D. (1991). Interpreting neural-network connection weights. *AI Expert* 6, 46–51.

Guillén, M. D., and Cabo, N. (1998). Relationships between the composition of edible oils and lard and the ratio of the absorbance of specific bands of their fourier transform infrared spectra. role of some bands of the fingerprint region. *J. Agric. Food Chem.* 46, 1788–1793. doi:10.1021/jf9705274

Halder, S., Dhawane, S. H., Kumar, T., and Halder, G. (2015). Acid-catalyzed esterification of castor (Ricinus communis) oil: optimization through a central composite design approach. *Biofuels* 6, 191–201. doi:10.1080/17597269.2015.1078559

Ibrahim, A. P., Omilakin, R. O., and Betiku, E. (2019). Optimization of microwave-assisted solvent extraction of non-edible sandbox (*Hura crepitans*) seed oil: a potential biodiesel feedstock. *Renew. Energy* 141, 349–358. doi:10.1016/j.renene.2019.04.010

Ighose, B. O., Adeleke, I. A., Damos, M., Junaid, H. A., Okpalaeke, K. E., and Betiku, E. (2017). Optimization of biodiesel production from *Thevetia peruviana* seed oil by adaptive neuro-fuzzy inference system coupled with genetic algorithm and response surface methodology. *Energy Convers. Manag.* 132, 231–240. doi:10.1016/j.enconman.2016.11.030

Ishola, N. B., Adeyemi, O. O., Adesina, A. J., Odude, V. O., Oyetunde, O. O., Okeleye, A. A., et al. (2017). Adaptive neuro-fuzzy inference system-genetic algorithm vs. response surface methodology: a case of optimization of ferric sulfate-catalyzed esterification of palm kernel oil. *Process Saf. Environ. Protect.* 111, 211–220. doi:10.1016/j.psep.2017.07.004

Ishola, N. B., Okeleye, A. A., Osunleke, A. S., and Betiku, E. (2019). Process modeling and optimization of sorrel biodiesel synthesis using barium hydroxide as a base heterogeneous catalyst: appraisal of response surface methodology, neural network and neuro-fuzzy system. *Neural Comput. Appl.* 31, 4929–4943. doi:10.1007/s00521-018-03989-7

Jaliliannosrati, H., Amin, N. A. S., Talebian-Kiakalaieh, A., and Noshadi, I. (2013). Microwave assisted biodiesel production from Jatropha curcas L. seed by two-step *in situ* process: optimization using response surface methodology. *Bioresour. Technol.* 136, 565–573. doi:10.1016/j.biortech.2013.02.078

Jisieike, C. F., and Betiku, E. (2020). Rubber seed oil extraction: effects of solvent polarity, extraction time and solid-solvent ratio on its yield and quality. *Biocatal. Agric. Biotechnol.* 24, 101522. doi:10.1016/j.bcab.2020.101522

Kamel, D. A., Farag, H. A., Amin, N. K., Zatout, A. A., and Ali, R. M. (2018). Smart utilization of jatropha (*Jatropha curcas* Linnaeus) seeds for biodiesel production: optimization and mechanism. *Ind. Crop. Prod.* 111, 407–413. doi:10.1016/j.indcrop.2017.10.029

Karmakar, B., Dhawane, S. H., and Halder, G., (2018). Optimization of biodiesel production from castor oil by Taguchi design. *J. Environ. Chem. Eng.* 6, 2684–2695. doi:10.1016/j.jece.2018.04.019

Karmee, S., Patria, R., and Lin, C. (2015). Techno-Economic evaluation of biodiesel production from waste cooking oil-A case study of Hong Kong. *Ijms* 16, 4362–4371. doi:10.3390/ijms16034362

Krisnangkura, K. (1986). A simple method for estimation of cetane index of vegetable oil methyl esters. *J. Am. Oil Chem. Soc.* 63, 552–553. doi:10.1007/bf02645752

Lisboa, P., Rodrigues, A. R., Martín, J. L., Simões, P., Barreiros, S., and Paiva, A. (2014). Economic analysis of a plant for biodiesel production from waste cooking oil via enzymatic transesterification using supercritical carbon dioxide. *J. Supercrit. Fluids* 85, 31–40. doi:10.1016/j.supflu.2013.10.018

Marchetti, J. M. (2013). Influence of economical variables on a supercritical biodiesel production process. *Energy Convers. Manag.* 75, 658–663. doi:10.1016/j.enconman.2013.07.039

Marchetti, J. M., and Errazu, A. F. (2008). Esterification of free fatty acids using sulfuric acid as catalyst in the presence of triglycerides. *Biomass Bioenergy* 32, 892–895. doi:10.1016/j.biombioe.2008.01.001

Merlin, A. Z., Marcel, O. A., Louis Max, A. O., Salem, C., and Jean, G. (2015). Development and experimental investigation of a biodiesel from a nonedible woody plant: the neem. *Renew. Sustain. Energy Rev.* 52, 201–208. doi:10.1016/j.rser.2015.07.027

Mozaffari, A., Emami, M., and Fathi, A. (2019). A comprehensive investigation into the performance, robustness, scalability and convergence of chaos-enhanced evolutionary algorithms with boundary constraints. *Artif. Intell. Rev.* 52, 2319–2380. doi:10.1007/s10462-018-9616-4

Muthu, H., SathyaSelvabala, V., Varathachary, T. K., Kirupha Selvaraj, D., Nandagopal, J., and Subramanian, S. (2010). Synthesis of biodiesel from Neem oil using sulfated zirconia via tranesterification. *Braz. J. Chem. Eng.* 27, 601–608. doi:10.1590/s0104-66322010000400012

Myers, R. H., Montgomery, D. C., and Anderson-Cook, C. M. (2016). *Response surface methodology: process and product optimization using designed experiments*. Chichester, UK: John Wiley & Sons.

Niu, S., Ning, Y., Lu, C., Han, K., Yu, H., and Zhou, Y. (2018). Esterification of oleic acid to produce biodiesel catalyzed by sulfonated activated carbon from bamboo. *Energy Convers. Manag.* 163, 59–65. doi:10.1016/j.enconman.2018.02.055

Ofoefule, A. U., Esonye, C., Onukwuli, O. D., Nwaeze, E., and Ume, C. S. (2019). Modeling and optimization of African pear seed oil esterification and transesterification using artificial neural network and response surface methodology comparative analysis. *Ind. Crops Prod.* 140, 1–16. doi:10.1016/j.indcrop.2019.111707

Ogbu, I. M., Ajiwe, V. I. E., and Okoli, C. P. (2018). Performance Evaluation of carbon-based heterogeneous acid catalyst derived from *Hura crepitans* seed pod for esterification of high FFA vegetable oil. *Bioenerg. Res.* 11, 772–783. doi:10.1007/s12155-018-9938-8

Okeleye, A. A., and Betiku, E. (2019). Kariya (*Hildegardia barteri*) seed oil extraction: comparative evaluation of solvents, modeling, and optimization techniques. *Chem. Eng. Commun.* 206, 1181–1198. doi:10.1080/00986445.2018.1550397

Oladipo, A. S., Ajayi, O. A., Oladipo, A. A., Azarmi, S. L., Nurudeen, Y., Atta, A. Y., et al. (2018). Magnetic recyclable eggshell-based mesoporous catalyst for biodiesel production from crude neem oil: process optimization by central composite design and artificial neural network. *Compt. Rendus Chem.* 21, 684–695. doi:10.1016/j.crci.2018.03.011

Oladipo, B., and Betiku, E. (2020). Optimization and kinetic studies on conversion of rubber seed (*Hevea brasiliensis*) oil to methyl esters over a green biowaste catalyst. *J. Environ. Manag.* 268, 110705. doi:10.1016/j.jenvman.2020.110705

Pasias, S., Barakos, N., Alexopoulos, C., and Papayannakos, N. (2006). Heterogeneously catalyzed esterification of FFAs in vegetable oils. *Chem. Eng. Technol.* 29, 1365–1371. doi:10.1002/ceat.200600109

Rashid, U., Anwar, F., Ashraf, M., Saleem, M., and Yusup, S. (2011). Application of response surface methodology for optimizing transesterification of *Moringa oleifera* oil: biodiesel production. *Energy Convers. Manag.* 52, 3034–3042. doi:10.1016/j.enconman.2011.04.018

Rincón, L. E., Jaramillo, J. J., and Cardona, C. A. (2014). Comparison of feedstocks and technologies for biodiesel production: an environmental and techno-economic evaluation. *Renew. Energy* 69, 479–487. doi:10.1016/j.renene.2014.03.058

Samuel, O. D., and Okwu, M. O. (2019). Comparison of Response Surface Methodology (RSM) and Artificial Neural Network (ANN) in modelling of waste coconut oil ethyl esters production. *Energy Sources, Part A Recovery, Util. Environ. Eff.* 41, 1049–1061. doi:10.1080/15567036.2018.1539138

Sani, Y. M., Daud, W. M. A. W., and Abdul Aziz, A. R. (2013). Solid acid-catalyzed biodiesel production from microalgal oil-The dual advantage. *J. Environ. Chem. Eng.* 1, 113–121. doi:10.1016/j.jece.2013.04.006

Sarve, A., Sonawane, S. S., and Varma, M. N. (2015). Ultrasound assisted biodiesel production from sesame (*Sesamum indicum* L.) oil using barium hydroxide as a heterogeneous catalyst: comparative assessment of prediction abilities between response surface methodology (RSM) and artificial neural network (ANN). *Ultrason. Sonochem.* 26, 218–228. doi:10.1016/j.ultsonch.2015.01.013

Selvaraj, R., Moorthy, I. G., Kumar, R. V., and Sivasubramanian, V. (2019). Microwave mediated production of FAME from waste cooking oil: modelling and optimization of process parameters by RSM and ANN approach. *Fuel* 237, 40–49. doi:10.1016/j.fuel.2018.09.147

Shan, R., Lu, L., Shi, Y., Yuan, H., and Shi, J. (2018). Catalysts from renewable resources for biodiesel production. *Energy Convers. Manag.* 178, 277–289. doi:10.1016/j.enconman.2018.10.032

Shanmuganathan, S. (2016). "Artificial neural network modelling," in *Studies in computational intelligence: an introduction*. Editors S. Shanmuganathan and S. Samarasinghe (Cham, Switzerland: Springer International Publishing), 1–14.

Conflict of Interest: The authors declare that the research was conducted in the absence of any commercial or financial relationships that could be construed as a potential conflict of interest.

NOMENCLATURE

ANN Artificial neural network
BBD Box Behnken design
FFA Free fatty acid
GA Genetic algorithm
MRPD Mean relative percent deviation
MAE Mean average error
MSE Mean square error
NSO Neem seed oil
R Correlation coefficient
R^2 Coefficient of determination
RMSE Root mean square error
RSM Response surface methodology
SEP Standard error of prediction